



# A Model of Black Sea Circulation with Strait Exchange (2008-2018)

Murat Gunduz<sup>1</sup>, Emin Özsoy<sup>2,3</sup>, and Robinson Hordoir<sup>4,5</sup>

<sup>1</sup>Institute of Marine Sciences and Technology, Dokuz Eylül University, İzmir, Turkey

<sup>2</sup>Institute of Marine Sciences, Middle East Technical University, Erdemli, Mersin, Turkey

<sup>3</sup>Eurasia Earth Science Institute, İstanbul Technical University, İstanbul, Turkey

<sup>4</sup>Institute of Marine Research, Bergen, Norway

<sup>5</sup>Bjerknes Centre for Climate Research, Bergen, Norway

**Correspondence:** Murat Gündüz (murat.gunduz@deu.edu.tr)

**Abstract.** The Bosphorus exchange is of critical importance for hydrodynamics of the Black Sea. In this study, we report on the development of a medium resolution circulation model of the Black Sea, making use of up-to-date topography, atmospheric forcing with high space and time resolution, climatic river fluxes and strait exchange enabled by adding the Bosphorus Strait with an artificial box on the Marmara Sea side. Particular attention is given to circulation, mixing, convective water mass formation processes compared with observations. The present formulation with temperature and salinity relaxed to the observed seasonal climatology of the Marmara box and open boundary conditions are found to enable Bosphorus exchange with upper, lower layer and net fluxes comparable to the observed range. This in turn enables to capture the trend of rapid climatic change observed in the Black Sea in the last decade.

## 10 1 Introduction

### 1.1 A Short Review of Black Sea Oceanography

The Black Sea is a part of the Old World's seas that has limited communication with the world ocean. Its unique oceanographic characteristics, natural and environmental history have been subject to a number of reviews by (Özsoy and Ünlüata, 1997, 1998; Oğuz et al., 2005; Kosarev, 2007; Sorokin, 2002; Grinevetsky et al., 2002; Vespremeanu and Golumbeanu, 2017).

15 Fluxes of momentum, water and buoyancy at the sea surface and at coastal and open boundaries dominate the hydrodynamics of semi-enclosed seas. Lateral fluxes, especially articulated in the Black Sea, by inputs from major rivers and the Bosphorus Strait exchange flows demand their adequate representation in this almost totally enclosed sea. Despite relatively small net flux on the order of 0.01 Sverdrup across the strait, strong coupling between the Bosphorus and the Black Sea is suggested by observations, in terms of circulation and mixing in either region.

20 Various modeling studies of the Black Sea circulation often with objectives similar to ours have considered realistic model configuration, initialization and time-dependent forcing elements aiming to generate results verifiable by observations. We skip



a review of the voluminous literature on stand-alone modeling of the Black Sea, while in the present study we aim to achieve coupling with Bosphorus Strait, extending the domain to include a portion of the Marmara Sea and also the Azov Sea, as will be detailed in the following sections.

## 1.2 Interaction with Straits

5 A unique regime of hydraulically controlled, turbulent and strongly stratified flow is well documented by observations in the Bosphorus (Gregg et al., 1999; Özsoy et al., 1995, 1996; Özsoy and Ünlüata, 1998; Özsoy et al., 2001; Gregg and Özsoy, 2002); including detailed assessments of the exchange fluxes (Jarosz et al., 2011a, b; Özsoy and Altıok, 2016a, b). Observations in the Marmara Sea have revealed two-layer stratified flow details, fluxes and circulation in this small internal sea (Ünlüata et al., 1990; Beşiktepe et al., 1993, 1994; Özsoy et al., 2016), connected to the Black Sea and Aegean Sea respectively by the  
10 Bosphorus and Dardanelles Straits.

Recent advances in modeling (İlıcak et al., 2009; Sözer and Özsoy, 2017a, b; Sannino et al., 2017) has provided details of the dynamics and mixing as well as the essential verification of the experimental synthesis of hydraulic controls, also providing evidence for "maximal exchange" special conditions satisfied in the Bosphorus. The Bosphorus Strait has been found to be a special environment that supports maximal exchange, even more strictly than the Gibraltar Strait for which the  
15 theory originally has been developed (Farmer and Armi, 1986, 1988). Later developments in modeling have enabled resolving the coupled dynamics of the Turkish Straits System (TSS) including the Bosphorus and Dardanelles Straits as well as the Marmara Sea in the model domain (Sannino et al., 2014, 2017; Aydoğdu et al., 2018a, b).

There is evidence that the interaction between the Black Sea and the TSS occurs in both ways and in different realms. For instance in the Black Sea, located in a strong climate gradient between the warm Mediterranean and continental Eurasia,  
20 an upper ocean cold water mass is formed in winter (the Cold Intermediate Layer, CIL), which formerly used to prevail throughout the year, although recent evidence (additionally in the present study) shows it to be fast disappearing. The CIL resides just above the halocline and provides fundamental contribution to static stability of the water column. At the same time, the CIL resides partially above the wide southern continental shelf (Figure 1) where it modifies the bottom Mediterranean plume exiting the Bosphorus into the Black Sea. The CIL further penetrates into the Bosphorus, where it influences turbulent  
25 mixing and entrainment between waters of Mediterranean and Black Sea origin, transformed towards the sharply stratified waters that emerge on the Marmara Sea. In this way the CIL, which is a product of convective mixing in the Black Sea, influences water mixed on the shelf and returned back to deeper layers of the Black Sea, also influencing Marmara Sea.

In correspondence to the above example of Black Sea influence on the TSS, the TSS also predetermines what would later become of its waters flowing to the Black Sea. The Mediterranean water plume exiting onto the Black Sea shallow continental  
30 shelf spreads along the shelf and canyon finally dipping down the continental slope, where it creates intrusions (Latif et al., 1991; Murray et al., 1991; Özsoy et al., 1993; Özsoy and Beşiktepe, 1995) leading to double diffusive convection (Özsoy et al., 1991; Özsoy and Beşiktepe, 1995; Kelley et al., 2003) and in extreme situations can penetrate throughout the Black Sea interior (Falina et al., 2017), interestingly found responsible for fast penetration of chemical signals such as the Chernobyl radiation fallout in the interior Black Sea (Rank et al., 1999; Özsoy et al., 2002; Delfanti et al., 2014). Novel features detected in the



region of spreading along canyon topography of the Black Sea shelf adjacent to the Bosphorus have led to detailed description of density currents along undersea channels with new hypotheses proposed on their turbulent dynamics (Dorrell et al., 2016, 2019). Based on the above literature, it is evident that the evolution of water properties and currents through the TSS influence mixing and water mass formation processes in the Black Sea shelf and continental slope boundary layers as well as the interior  
5 region.

As regards coupled modeling of Black Sea and the TSS, we can quote Sannino et al. (2017) results showing the changes in circulation of the Marmara Sea in response to net flows through the Bosphorus, finally leading to switching of the modes of circulation in response to extreme cases of flow blocking in the Bosphorus. Similarly Stanev et al. (2017) showed significant changes in coupled circulations of the Black Sea and Marmara Sea in response to changes in flow through straits.

## 10 2 Model Configuration

We aim to closely reproduce the circulation and hydrography of the Black Sea during the last decade by developing a unique high-resolution model prototype that relies on high fidelity forcing data sets available today on atmospheric reanalysis and climatological riverine fluxes, also considering coupling with the external ocean by including a "Marmara box" and the Bosphorus Strait in communication with the Black Sea. In this respect, the model aims truthful reproduction of the interplay between  
15 thermo-haline circulation, water mass formation dynamics and inter-basin exchange in coupled fashion. Our renewed effort aims to improve the great number of previous modeling studies that have simulated some characteristics of the Black Sea circulation without reference to Bosphorus exchange, thereby to close gaps in predictability of the physical response of this complex basin on scales from days to a decade by introducing the essential strait coupling.

It is with worth noting that the original configuration of NEMO version 3.3.1 we used earlier had horizontal resolution  
20 of  $1/12^\circ$  grid and 42 vertical levels. Having a coarser grid, using an earlier version of GEBCO topography, Levitus gridded climatology for initial conditions, atmospheric fluxes based on ECMWF ERA-interim reanalyses and only major rivers Danube, Dniestr, Dniepr and Don included, the strait exchange not sufficiently representative, an update seemed in order as we moved to the present model configuration for improved results.

### 2.1 Model Domain, Grid and Bathymetry

The present Black Sea circulation model (BSEA) is based on the NEMO version 4.0 (Madec, 2008) with advanced features of a community model accounting for complex physics of the marine environment. The model domain between  $40.69^\circ$ - $47.30^\circ$  N and  $27.43^\circ$ - $42.00^\circ$  E includes the deep Black Sea basin (max depth: 2178 m) together with the shallow Azov Sea (depth 10m) in the north and the Marmara Sea in the south. The bathymetry for the model displayed in Figure 1 is based on the General Bathymetric Chart of the Oceans GEBCO08 grid version 20100927 released in 2010, which we find the most up-to-date and  
30 accurate data set for the Black Sea, with 30 arc-seconds resolution.

The model domain includes Azov Sea in the north, the shallowest sea in the world, with a maximum depth of 14m in the middle, separated from the main body of the Black Sea by the narrow Strait of Kerch. The river Don joins Azov Sea at its head,

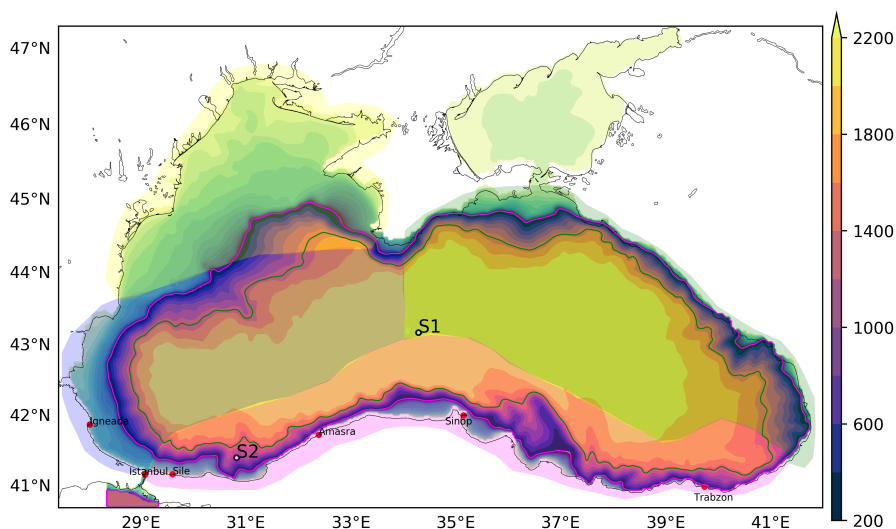


**Figure 1.** Model domain and bathymetry. The polygons show three subregions of the Black Sea (namely "east", "west", "rim") used to sample the ARGO floats. Five tide gauges along the Turkish coast are shown by red dots (İğneada, İstanbul, Şile, Amasra, Sinop and Trabzon). Contours in the range 100-2300 m (contour interval 200 m) correspond to the colour scale on the right. Contours in the depth range 0-100 m (contour interval 10 m) are superimposed with different colour scale (not shown) and 100m contour marked in magenta. Two stations (S1 and S2) shown in white dots are used to construct time series plots.

while the river Kuban joins near the Kerch Strait. The bathymetry and width of Kerch Strait has been artificially increased in the model (Figure 1), in order to have unobstructed exchange with the Black Sea, necessitated by the high river discharges into this relatively small, shallow domain with very sensitive response to wind stress forcing.

In order to represent the Bosphorus exchange flows coupled to Black Sea, an artificial box representing the Marmara Sea and the Bosphorus Strait have been added to the domain. The Marmara box is bounded by the northern coast of the Marmara Sea including the Bosphorus entrance and three open boundaries (i) along 40.74° N (ii) 28.403 °E (iii) 29.28° E, with the depth limited to 1200m at the bottom and true bathymetry elsewhere.

The model nominal grid resolution is  $\Delta x \equiv \Delta y \equiv 2.5\text{km}$  ( $0.03133^\circ$  longitude by  $0.02286^\circ$  latitude) along both horizontal directions resulting in an equally spaced horizontal grid of dimension 466 x 280, and a vertical grid with 60 z-levels of partial steps configuration. The resolution of the vertical grid has been adjusted so as to be compatible with the topography and density variations. The minimum vertical grid size of 2m at the surface, increasing to about 3m at a depth of 40m, then to about 10m at a depth of 110m is designed to adequately represent the surface mixed layer which is typically shallower than 25m, and the main halocline which is usually shallower than 100m in the Black Sea. There are 20 levels in the first 50m of depth, followed by 10 in the next depth range until 100m (Figure 2). The wide shelf areas especially of the western Black Sea typically limited by the 100m depth contour at the shelf edge are sufficiently resolved by this vertical grid. The model integration was carried out with a baroclinic time step of  $\Delta t_i = 240\text{s}$ .

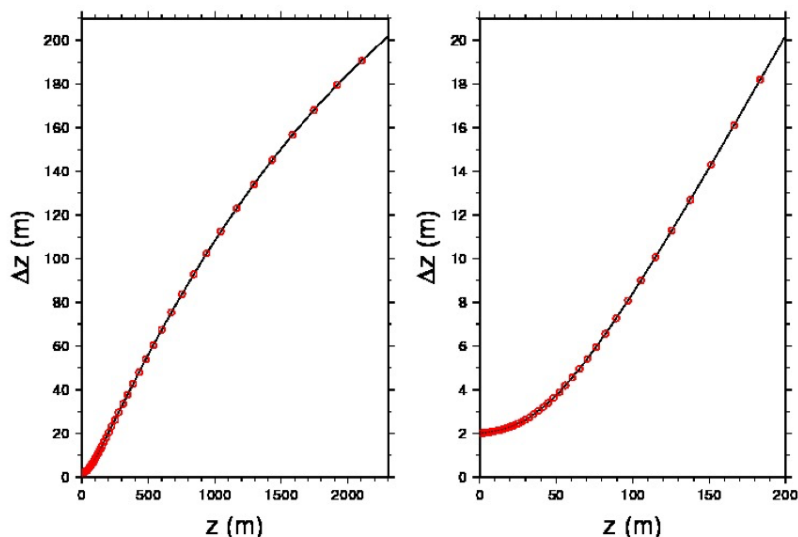


**Figure 2.** Model vertical grid spacing  $\Delta z$  (meters) as a function of the vertical coordinate  $z$  displayed for (a) maximum depth of 2300m, (b) in the upper 200m.

The model bathymetry represented in Figure 1 has been moderately smoothed using scale selective filters, satisfying the slope criterion of ROMS (Song and Haidvogel, 1994) so as to have  $rx0 = \max(\Delta h/h) < 0.3$  between any neighboring grid points, where  $h$  is the depth.

In regard to the Bosphorus coupling, it should be clear that the present horizontal and vertical grid resolution needed to represent the complicated bathymetry at the Strait is less than what would be needed. It is therefore to be expected that the present configuration insufficient resolve strait topography would not be capable to reproduce the full range of nonlinear dynamical behavior of the Bosphorus Strait. The present choice is made in recognition of this fact in order to include strait coupling to the lowest order of approximation, saving the required effort for the future.

## 2.2 Parametrization

10 The numerical values of the horizontal viscosity length and velocity are taken  $1km$  and  $0.1m/s$  respectively. The horizontal diffusive length scale and velocity are  $2km$  and  $0.01m/s$  respectively. Values for vertical eddy viscosity and eddy diffusivity are selected as  $A_v m = 1.e-7m^2/s$  and  $A_v t = 1.e-8m^2/s$ . Turbulent Kinetic Energy (TKE) turbulent closure scheme (Blanke and Delecluse, 1993) is applied in the vertical with default settings in NEMO version 4.0 configuration. Bi-laplacian diffusivity schemes are used for both tracer and momentum.



**Table 1.** Climatological monthly river runoff for major Black rivers (m<sup>3</sup>/s)

River	Annual	Jan	Feb	Mar	Apr	May	Jun	Jul	Aug	Sep	Oct	Nov	Dec
Danube	6365.0	5818.6	6091.6	7215.7	8397.7	8754.2	8144.7	6976.1	5405.6	4607.1	4355.1	4893.3	5719.8
Dnieper	1630.8	1505.0	1757.6	1839.1	2723.8	3180.6	1777.2	1162.7	1035.5	925.1	1077.2	1221.9	1364.2
Don	850.7	345.3	295.2	292.2	482.2	1284.9	2913.6	1532.6	1144.6	827.7	465.8	335.0	289.4
Rioni	409.7	303.3	346.3	431.1	654.8	611.9	535.2	428.2	326.4	240.9	294.6	357.6	386.2
Kuban	350.8	268.2	240.6	318.6	380.2	548.7	524.3	473.2	371.3	288.0	256.8	233.1	306.1
Dniestr	326.3	180.2	256.3	479.0	535.1	400.2	437.4	413.6	303.4	250.8	215.1	226.9	217.6
Sakarya	217.3	301.9	306.7	332.7	304.2	206.3	165.3	138.4	124.9	126.2	139.3	246.2	216.2
Kizilirmak	202.2	212.9	255.4	328.4	308.2	231.2	157.0	118.2	123.8	147.4	167.6	173.4	202.6
Southern Bug	110.4	86.8	124.0	258.6	215.2	86.3	71.0	89.6	66.5	67.3	88.5	85.2	85.8
Kamtehiya	22.4	30.4	43.0	45.7	32.3	25.8	20.4	11.2	8.4	8.3	6.6	14.4	22.4

### 2.3 River Input

The inputs of fresh water from major rivers, Danube in Romania, Dniester, Southern Bug and Dnieper in the Ukraine, Don, Kuban in Russia, Rioni in Georgia, Kizilirmak and Sakarya in Turkey, and Kamtehiya in Bulgaria have been accounted for, by using climatological monthly discharges reported by the RivDIS data base. Climatological monthly discharges of the rivers are given in Table 1.

The total annual river inflow represented with 11 rivers in the model amounts to  $10570\text{m}^3/\text{s}$  ( $= 333\text{km}^3/\text{yr}$ ). Kara et al. (2008) have found little difference in comparing different sources of river runoff, including a budget based on 6 major rivers of the Black Sea, totaling  $9160\text{m}^3/\text{s}$  ( $= 289\text{km}^3/\text{yr}$ ).

More importantly, additional land-based sources of water other than rivers may be more important, though often neglected. If the overland runoff were to be taken into account, the total freshwater inputs apparently would increase by another 30%, amounting to a total of  $13825\text{m}^3/\text{s}$  ( $= 436\text{km}^3/\text{yr}$ ) according to Black Sea data displayed at the GRDC web portal ([http://geoportal.bafg.de/mapapps/resources/apps/GRDC\\_FWF/index.html?lang=en](http://geoportal.bafg.de/mapapps/resources/apps/GRDC_FWF/index.html?lang=en)) “fresh water fluxes to the world oceans”, although the monthly data for the overland flows could not be separately accessed, and therefore not included in our account.

According to the same source (GRDC), the total freshwater runoff has significant inter-annual variability. As it can be observed in Figure 3, the total discharge of freshwater into the Black Sea by rivers plus the overland runoff varies by almost two fold from one year to the other. Considering seasonal variability within each year this variability is even higher on inter-annual time scales, as demonstrated by Özsoy and Ünlüata (1998), based on long term data provided by Simonov and Altman (1991).

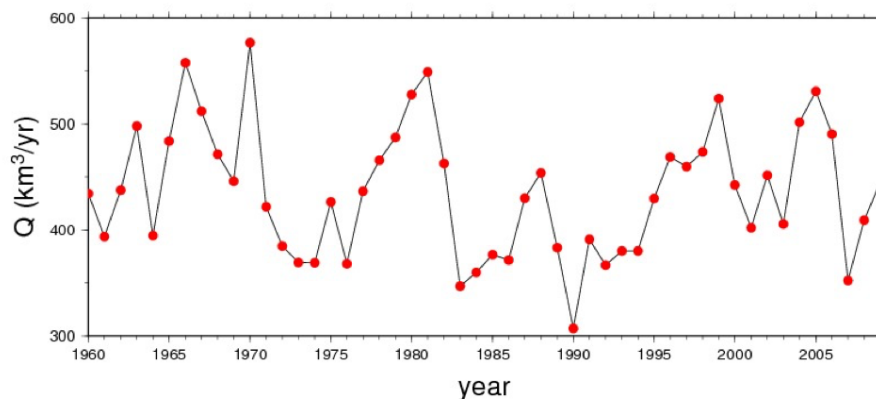


**Figure 3.** Inter-annual variations of mean annual freshwater inflow to the Black Sea – source: GRDC ([http://geoportal.bafg.de/mapapps/resources/apps/GRDC\\_FWF/index.html?lang=en](http://geoportal.bafg.de/mapapps/resources/apps/GRDC_FWF/index.html?lang=en)).

The Danube river discharge monitored since last two centuries clearly displays this great interannual / interdecadal variability (Bondar, 1986; Sur et al., 1996). The air sea exchange of water by precipitation and evaporation adds further variability to the water exchange.

From the above discussion it is obvious that the water budget of the Black Sea is highly variable on inter-annual and seasonal time scales because of climatological factors and is influenced by insufficient accounting of all freshwater sources such as overland runoff, implying that the model response to freshwater inputs is expected to vary greatly at any instance. For the moment we use the climatological monthly river fluxes as lateral sources of freshwater in the model, although we fully recognize the future need to account for the net water exchange regulated by the Bosphorus Strait.

## 2.4 Open Boundary Conditions

10 Within the Marmara box domain external to the Black Sea, temperature and salinity were relaxed to climatological values, which were a function of depth only, along a buffer zone that is 5 grids wide in parallel to the open boundary, only leaving out a very small area near the Bosphorus entrance quickly adjusted to the rest of the domain shortly after initialization. The depth and time dependent values imposed at the open boundary were obtained from historical data sets as daily climatology, by averaging over corresponding dates of years with suitable smoothing and static stability checks among available archives  
15 of CTD data at IMS-METU. The averaging of the data that was finally applied at the Marmara box was done over the entire Marmara Sea for increased statistical reliability of the observational daily T,S profile time series, which are shown in Figure 4. The data were used to initialize and later to relax for the properties within the Marmara box.

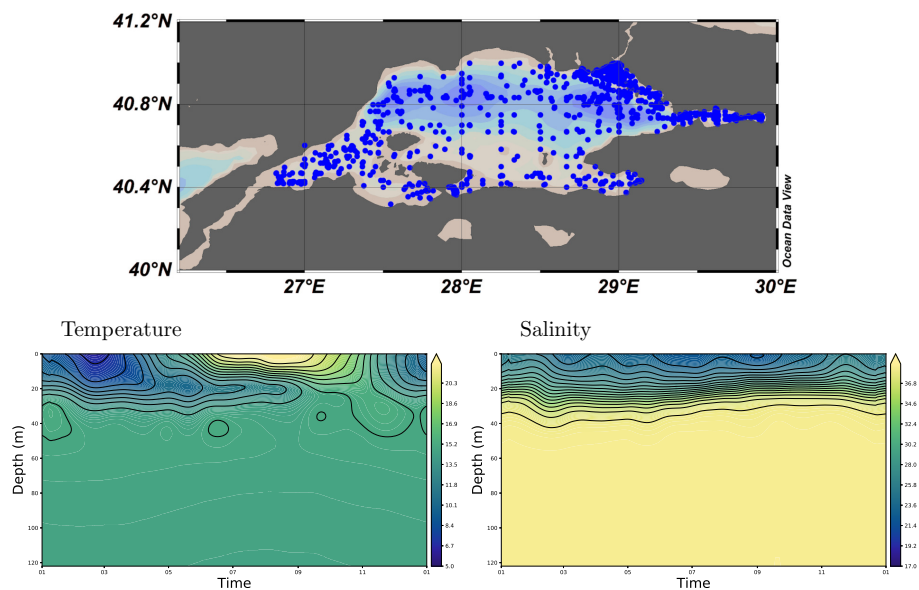


**Figure 4.** Time series of daily climatological salinity (left) and temperature (right) profiles and location of the CTD stations (top) applied for relaxation at the Marmara box shown in the 1.

## 2.5 Initialization and Atmospheric Forcing

The initial conditions of the model are constructed from intercalibrated temperature and salinity data from the 1992 CoMSBlack cruise, a multi-national collaborative oceanographic survey which quasi-synoptically covered the entire Black Sea in maximum possible extent and detail (<http://www.grid.unep.ch/bsein/descript/cblack92.htm>), carried out during 2-26 July 1992 by five  
5 research vessels from the riparian countries, as quoted in Oğuz et al. (1993) and (Sur et al., 1994, 1996). The data obtained from a total of 394 hydrography stations at nominal spacing of 20' (=1/3°) in longitude and latitude have been screened to eliminate few stations contributing to anomalous properties in the analyzed fields. The objectively analyzed temperature and salinity fields at the surface (model level 1) and at a depth of 89m (model level 28) respectively are shown in Figure 5.

The model was initialized with the July 1992 analysis fields substituted for the July 1, 2008 initial conditions and run for  
10 about 10.5 years from 01/07/2008 to 31/12/2018, subject to the atmospheric forcing and surface and lateral flux boundary conditions as specified above. The substitution of the July 1992 analysis for initial conditions is misplaced by more than two decades from the modeling period, but it was justified in the absence of other reliable initial data, providing the best possible synthesis of the entire basin hydrography ever made. Although the model would need a few years of spin-up time for adjustment to the initial and boundary conditions, the adjustment run was not carried out, as the objective of model performance testing  
15 prevailed. Results obtained so far illustrate rather fast adjustments of the model fields without much vertical displacements or oscillations encountered, although this remains to be finally tested in the future by persistence runs or multi-decadal runs from actual initial conditions. We choose to start from a representative initial condition, albeit the fact that it is misplaced in time,

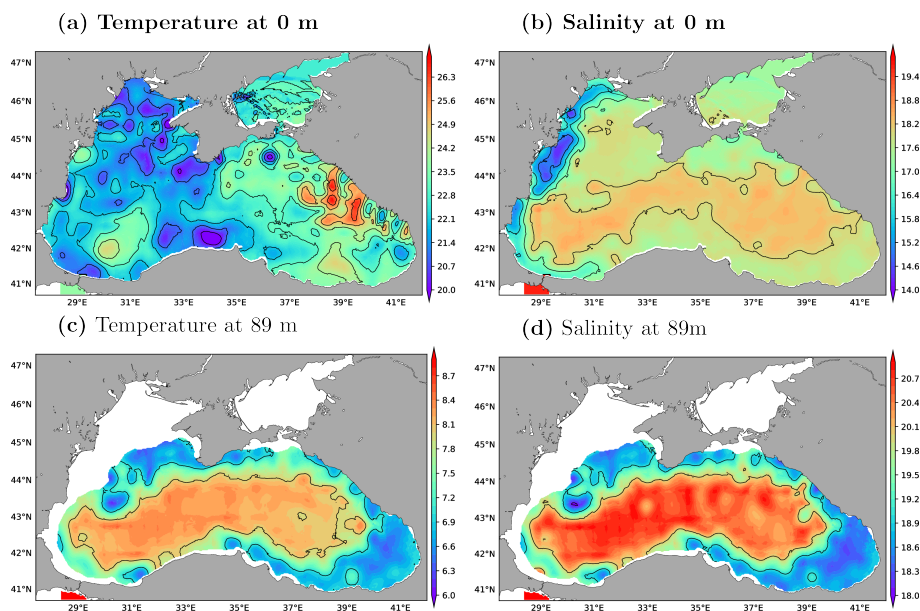


**Figure 5.** Model initial conditions of temperature (lhs) and salinity (rhs) at the surface (upper row) and at a depth of 89m (lower row), based on the objective analyses of data from a total of 394 CTD measurement stations obtained during the July 1992 CoMSBlack cruise.

and allow the model dynamics with realistic forcing alone to set up the circulation, without any climatological adjustments of the initial or evolving fields.

Surface fluxes are computed using the core algorithm of NEMO, based on the European Centre for Medium-Range Weather Forecasts (ECMWF) atmospheric reanalysis product ERA5 Re-Analysis data set. The ERA5 high space and time resolution atmospheric data at 1 hr intervals and 31km horizontal grid spacing of the atmospheric model is interpolated on-the-fly by the NEMO ocean model and applied at the surface using the COARE 3.5 bulk formulae (Madec, 2012).

First model runs have been carried out with the ERA5 precipitation. However, the comparison of model salinity with ARGO floats showed a difference in trends between model and observations at the end of model simulation. Detailed analysis have revealed that the ERA5 precipitation is significantly lower than the ERA-Interim precipitation in the Black Sea with a ratio of about 2. Therefore, we decided to replace the ERA5 with ERA-Interim precipitation for the rest of model runs, keeping the source for other variables the same.

### 3 Model Evaluation

#### 3.1 Bosphorus Fluxes

The extension of the Black Sea to the Marmara "box" through the Bosphorus Strait aimed to represent strait and basin coupling in the model. This is achieved through relaxation of properties to climatological daily stratification in the box and Flather



**Table 2.** Water Transport

	analysis		observations		Model result
	(1)	(2)	(3)	(4)	
	South/North	mid-strait	South/North	South/North	South/North
upper layer	-653/-603	-540	-420/-395	-444/-374	-508/-492
lower layer	353/303	115	249/255	333/252	298/281
net	-300/-300	-425	-171/-140	-111/-122	-209/-210

(1) Ünlüata et al. (1990); (2) Özsoy et al. (1996); Özsoy and Ünlüata (1998); (3) Altıok and Kayısoğlu (2015); (4) Jarosz et al., 2011b, a)

boundary conditions Oddo and Pinardi (2008) applied at the Marmara box open boundaries. Although the Flather open boundary conditions imply that the sea surface height and normal velocity are adjusted to values specified at the boundary with some radiation of the disturbances, we set these to zero and let the model calculate them in accordance with wave radiation and with the help of upstream boundary conditions for outflowing components. As the temperature and salinity near the boundary (effectively in the greater part of the small box) are relaxed to climatological boundary conditions, the outflow and inflow at the artificial boundaries are verified to approach approximate volume conservation apart from a small inconsistency, but ensuring two way exchange at the Bosphorus approaching realistic values with a net barotropic component.

Comparison of the time series for upper, lower layer and net fluxes in the Bosphorus Strait obtained from the model and observations from August-2008 to Jan -2009 are superposed in Figure 6. The experimental fluxes are based on Jarosz et al. (2011b) measurements. We observe that the model results are in the same range of mean fluxes obtained from observations, although there are differences in the oscillatory part of the signals. We also observe that the lower layer fluxes are in better agreement between the model and observations, while the upper layer fluxes outwards from the Black Sea are less compliant, most likely because the outflow is directly related to the surface water balance of the Black Sea.

The various historical estimates of Bosphorus fluxes based on mass budgets and direct observations in the literature, re-evaluated by Özsoy and Altıok (2016a) are listed in Table 1, compared with the model computed values in the last column.

It is noted in Figure 6 that the longer term model fluxes of the upper, lower layer and net flows in magnitude and direction are in better agreement with the observations, while the short-term components on the order of few days to a week have greater amplitude in the observations compared to the model, possibly because of the insufficient model resolution to fully duplicate hydraulically controlled, turbulent flow dynamics of the strait at this resolution, as remarked earlier in the model configuration section.

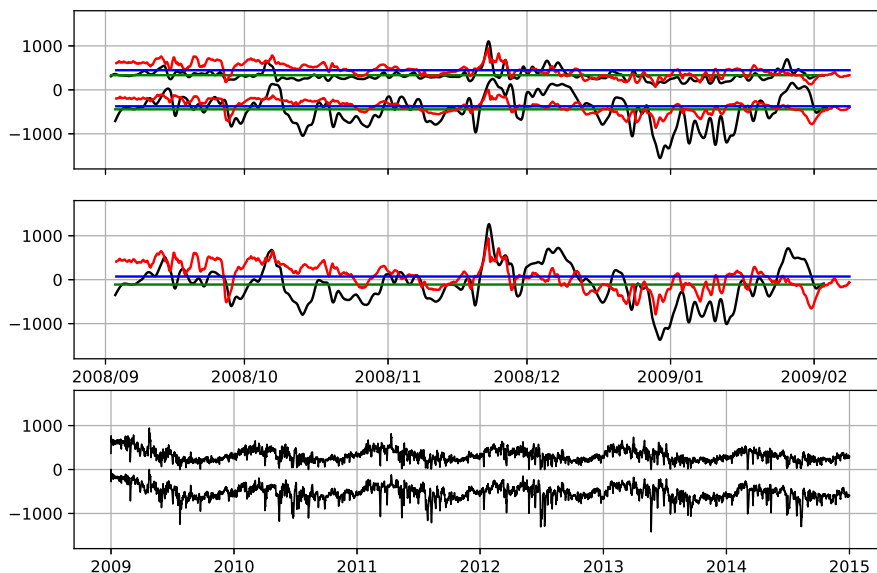


**Figure 6.** Time series of water transport at Bosphorus Strait. Upper panel: Upper and lower fluxes from the model (red line) and from observations (black line) compared for the August-2008 to Jan -2009 period. Middle panel : Net water transport from model (red line) and observation (black line). Lower panel : Upper and lower layer fluxes from the model for the entire model run period.

### 3.2 Comparison with ARGO Floats

Model generated temperature and salinity profiles were compared with the available ARGO floats data in the Black Sea. For this purpose, the model results were sampled at each ARGO float location and depth within each of the polygons shown in Figure 1. Figure 7 shows profiles of salinity (left column) and temperature (right column) averaged over the three sub-regions.

5 To construct this plot, a total number of 8167 profiles were used for "east" region, 6230 profiles for the "west" region and 5820 profiles for the "rim" region. Model results are shown in color shading in the background, and ARGO samples are contoured in black. There is good correlation between model results and ARGO salinity for each of the three sub-regions, indicating that the model is able to reproduce salt conservation under the created mass fluxes and mixing events during the model integration period. The red line shows the 21 salinity contour obtained by the model.

10 Although model results closely follow observations, with amplitude of the mixing events coinciding remarkably well, it seems that there is a slight increase of the 21 salinity depth especially in the eastern sub-region after 2017. The evolution of temperature in the model versus observational data shown on the right hand side of Figure 7 leaves little doubt that the model is able to reproduce observed variations remarkably well over a decade-long integration.

15 The model performance evaluated on its ability to reproduce CIL water mass and in capturing the thermocline depth, seems also satisfactory. The model temperature is shown in background color while contour lines show incremented values of 7 to 8.5°C for the ARGO (black line) and for the model (red line). It is seen that the model is able to generate the CIL water for each

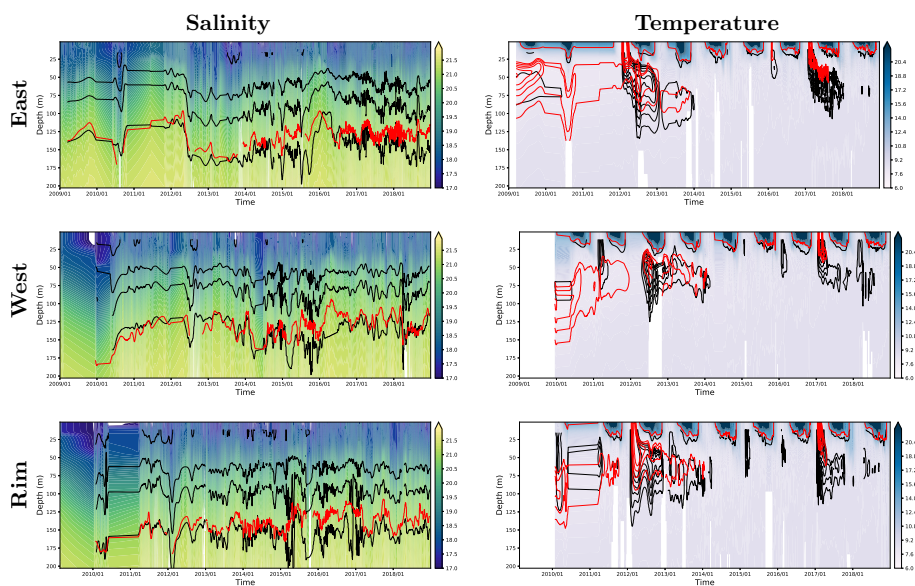


**Figure 7.** CTD profiles of salinity (left column) and temperature (right column) for the three subregions shown in the Figure 1. Top panel for the "east" region, middle panel "west" region and bottom panel "rim" region. Model results were shown as background fill image for each figure. Argo and model results were also shown in contour line (17 to 22 for salinity, 7 to 8.5 and 15 ° C for the temperature), black line for the argo, red line for the model.

of the investigated sub-regions. The model is also able to reproduce the interannual variation of the thermocline. The contour at the upper 50m marks the 15 ° C temperature (red line model, black line ARGO) for reference.

In Figure 8, the time series of ARGO float samples and model temperature at 25 m depth are compared for those samples in the east, west and rim regions. Considerably good visual agreement between the observed and modeled temperature suggests  
5 that the surface heat flux in the model and mixed layer dynamics are appropriate for maintaining the surface temperature close to reality over the last decade.

In Figure 9 both the observed and the model salinity time series at 25 m depth display increasing trends over the 10 year period, while the model trend appears slightly larger than the observed one in all regions, but especially in the east. These trends are evidence that increased environmental change are in due course in the Black Sea as has been recently shown by  
10 (Stanev et al., 2017). We also note that the trend in model salinity has been significantly reduced by choosing ERA-interim precipitation in place of ERA-5 since the latter source was found to result in much smaller total precipitation and had produced higher salinity trend as well as a much reduced net transport through the Bosphorus (not shown), as discussed in the earlier sections.

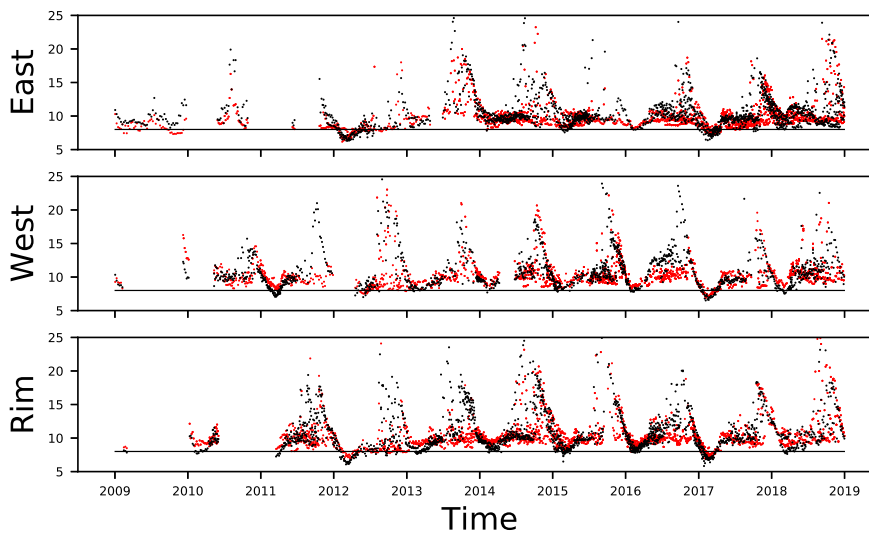


**Figure 8.** Time series of model and argo temperature at 25 m sampled over the three regions shown in the Figure 1. upper: east, middle:west, lower:rim. Black dots from argo floats, red dots from model results.

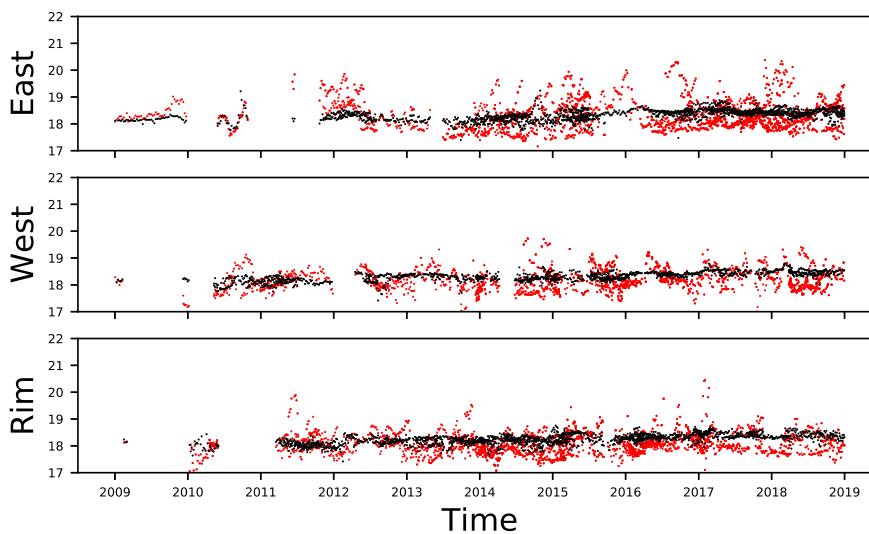


**Figure 9.** Time series of model salinity at 25 m sampled over the three regions shown in the Figure 1. upper: east, middle:west, lower:rim. Black dots from ARGO floats, red dots from model results.

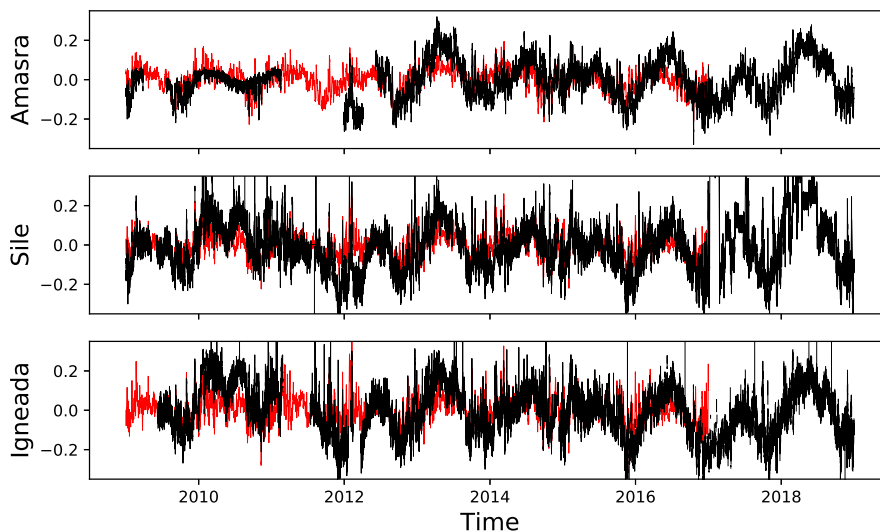


**Figure 10.** Time series of sea surface height anomaly for the three tide gauge stations shown in the Figure 1. Upper: Amasra, Middle: Şile, Lower:İğneada. Model result is black line and tide gauge record is red line.

### 3.3 Comparison with the Tide Gauges

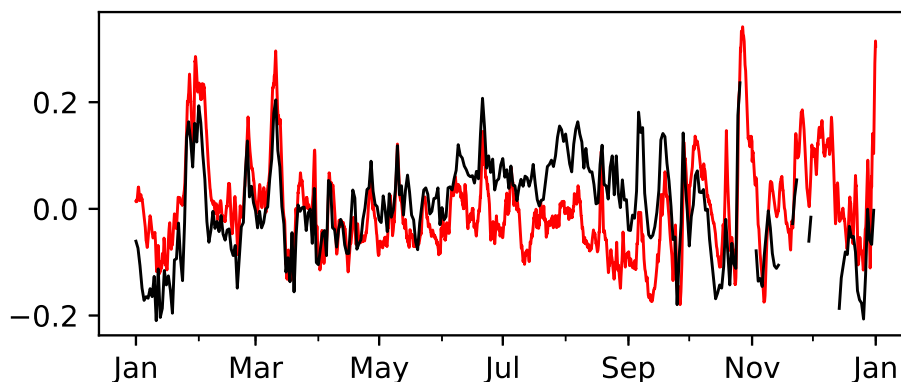
Model generated sea surface height (SSH) was compared with the six tide gauges located along the western and southern Black Sea coast. For this purpose, SSH anomaly was computed for model and observations, given in Figure 10 for the run period. The model results are in general agreement with the observations especially at higher frequencies, except for the irregular seasonal variation of greater amplitude evident in the observations.

It is yet immature to explain this difference at present, given the possible deficit in closing the Black Sea water budget, e.g. by imposing climatological river discharges rather than actual, inaccuracies in precipitation and evaporation estimates, as well as model approximations of the free surface. Especially in regard to the latter, first we note that we have used the linear free surface assumption in the present runs, with plans to use the nonlinear free surface option in future runs. Secondly, the seasonal, spatially variable steric component of sea level in the Black Sea reported to have an amplitude on the order of 2 cm by (Tsimplis et al., 2004), but estimated to reach 6 cm at some locations by (Arkhipkin and Bereznoi, 1995), often are not properly accounted for by ocean circulation models at present. All these factors could have contributed to the difference in model and observed SSH anomalies .

Samples of annual comparisons between model and observed SSH anomalies in Figure 11 are more optimistic however, as they display better agreement between the higher frequency components in the range of daily to weekly and fortnightly oscillations, leaving aside the longer term and seasonal, possibly steric or fresh-water induced components.



### (a) Igneada 2014



### (b) Amasra 2017

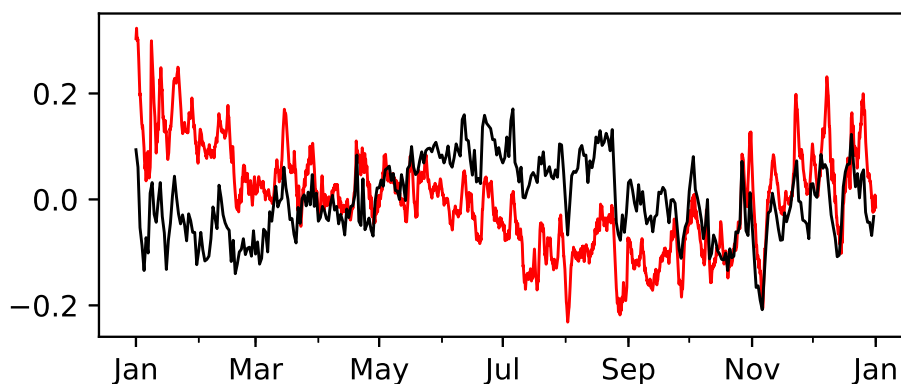


**Figure 11.** Time series of sea surface height anomaly for three tide gauge station shown in the Figure 1. Upper: Amasra, Middle: Sile, Lower: Igneada. Model results is black line and tide gauge results are red line.

## 4 Initial results and applications

### 4.1 Circulation and mixing

The main characteristics of the Black Sea general circulation have been rather well established based on a multitude of experimental investigations, numerical modeling studies and reviews (e.g. (Stanev, 1990; Oğuz et al., 1993; Oğuz and Malanotte-Rizzoli, 1996; Özsoy and Ünlüata, 1997, 1998; Sarkisyan and Sündermann, 2009)). Our purpose is not to provide an exposé of the seasonal circulation expected, but rather to briefly demonstrate model realizations of well known circulation features through some examples.

In Figure 12 we present an exemplary selection of monthly average circulation and temperature fields at the surface (left) and at depth of 50 m (right) developed from December 2011 to March 2012. It can be noticed by from the plots on the



right hand side that downwelling exists all along the continental slope region of the closed basin of the Black Sea, where higher temperature near the periphery occur and where the cyclonic rim current also roughly resides. In fact a well-developed cyclonic surface circulation with meandering currents and anticyclonic eddies along the periphery of the deep basin are evident. On the left hand side, the greater temperatures in December are reduced until March, where a cold patch surviving in the north central part of the western basin is advected to the south eastern basin near the Bosphorus, while at the same time cold water is formed in the shallow northeast shelf and the Azov Sea, preserved there until March. The cold water on the shelf is later seen in February and March to leak out of the northwest shelf area to appear on the slope of the Danube delta at 50m depth and circulated around the basin. Well noted circulation elements of the Sevastopol eddy trapped west of the Crimean peninsula and Batumi eddy in the southeastern corner are in development.

10 In Figure 13 we present an exemplary selection of monthly average surface currents for the months of July, September 2011, February, May 2012 (left) and July, September 2014, February, May 2015 (right), where rapid changes occur in terms of the strength of the rim current, the creation and destruction of eddies, the propagation of eddies along the rim current and across the basin, filaments of jets separating from the main rim current and their roles in weakening and re-organization of ordered fast currents following the periphery, which show a series of dynamic events that rapidly change the structure and sequence of circulation elements that are all too important in the short and long term changes in the environment under the evolving climate.

## 4.2 Time Evolution at Stations

We examine the temperature and salinity evolution in the system. In particular, we examine in Figure 14 the upper ocean properties at stations 1 and 2 of Figure 1, to observe the typical seasonal / inter-annual response pattern of the forced system started from the initial condition during the relatively short period of about 10 years.

At station 1 at the very center of the basin, in Figure 14.a, we see cycles of summer warming that develops thermal stratification within the mixed layer region up to a depth of about 25-30 m followed by winter time convective mixing. The Cold Intermediate Layer (CIL) conveniently defined as the layer of intermediate depth water of temperature less than  $8^{\circ}\text{C}$  is present at depths of up to 80 m below the mixed layer in the initial conditions imposed on 1 July 2008. The CIL survives until the summer of 2012 and disappears afterwards at this station. While convection seems to occur every winter, fresh cold intermediate water contributing to the core with  $T < 8^{\circ}\text{C}$  principally occurs only in the winter of 2012, in fact when cold water with  $T < 7^{\circ}\text{C}$  evidently creating convective overturning extends from the surface down to the core of the CIL at about 40 m. In the following years the cooling seems to be reduced with new cold water formed, but evidently not cold enough as the CIL has been characterized in the not so distant past, and intermediate waters in later years undergo warming. The salinity time series in Figure 14.a shows the halocline at depths of around 50m, at just about the CIL lower depth limit. Both the temperature and the salinity records show many fine scale features and oscillations associated with the eddying and small-scale motions.

At station 2 (Figure 1) near the southern boundary of the basin, in Figure 14.b, we observe that the thermal and salinity stratification are much deeper than the central basin station 1, evident by the increased depth of the halocline to about 80 m, and the depth of the mixed layer also deeper compared to the central region. The deeper structure near the coast, in comparison

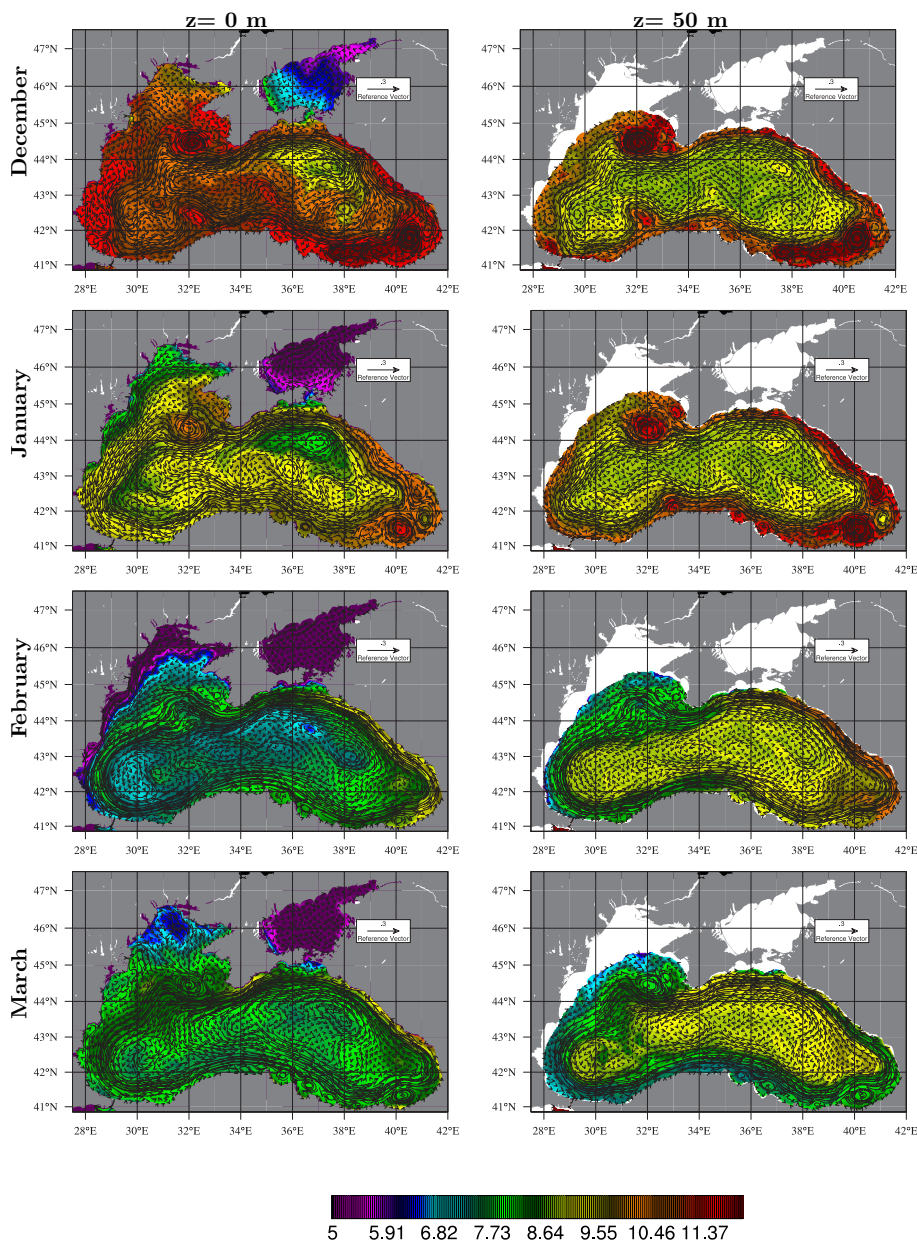


**Figure 12.** Monthly average currents and temperature at the surface (left) and at depth of 50 m (right) developed from December 2011 to March 2012 (ordered down the page).

to the central area of doming in the Black Sea are also evident in (Figures 12 and 13). The CIL is thicker at the near coastal station 2, its lower limit reaching a depth of about 100m at this mainly anticyclonic region. The convective overturning in the

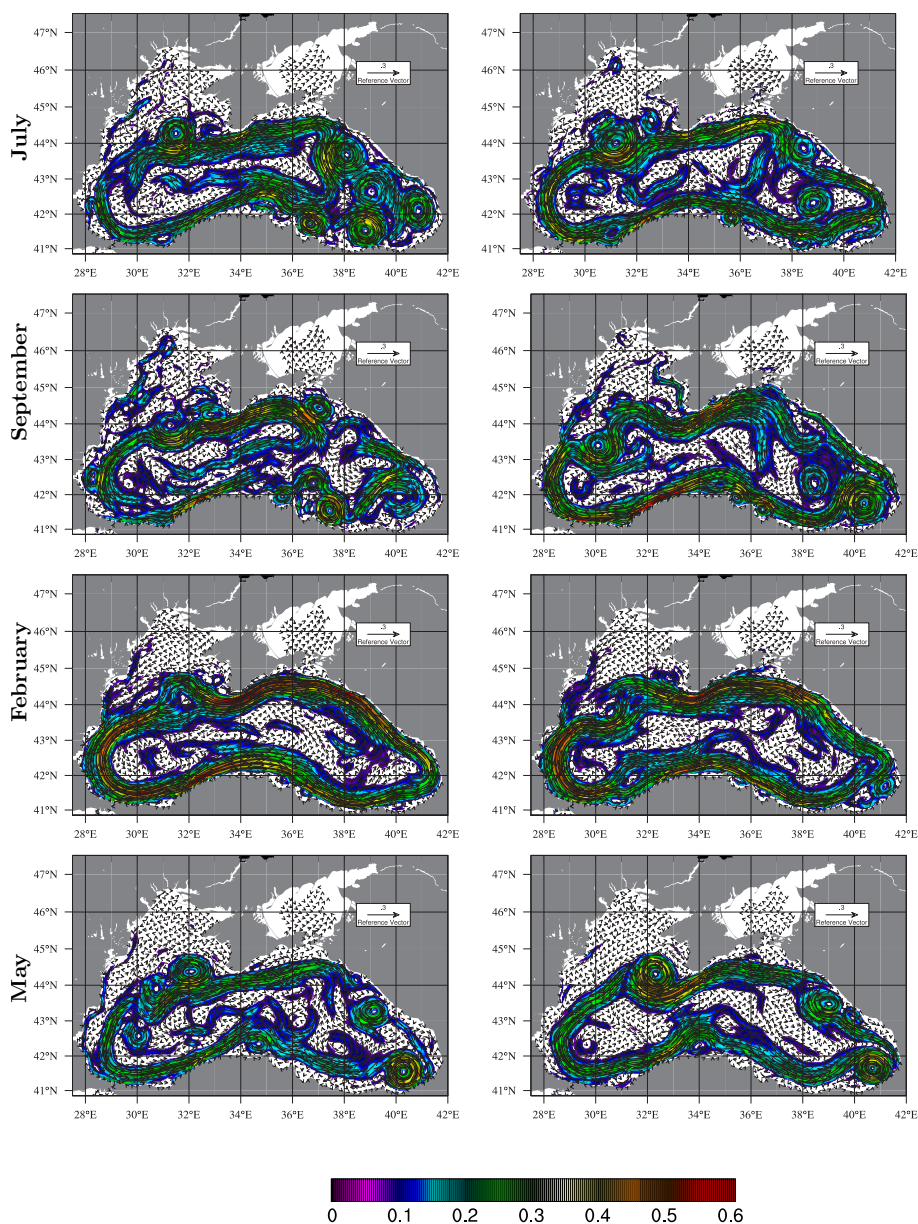


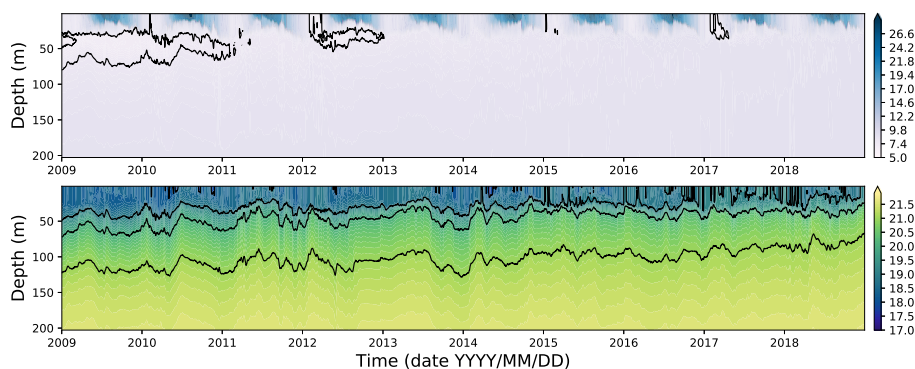
**Figure 13.** Monthly average current vectors and magnitude in color shading for the months of July, September 2011, February, May 2012 (left) and July, September 2014, February, May 2015 (right) (ordered down the page).

winter of 2012 therefore also becomes deeper, reaching the lower depths of the CIL core. The increased oscillatory behavior as compared to station 1 is a result of the meso-scale eddying motions of the rim-current effective at the periphery of the basin.

The abundance of CIL in the initial conditions maintained for the first two years contrasts with the single event of cold intermediate water formation in 2012, and the weaker event in 2017. The reduced convection events in recent years both in



### (a) Station 1



### (b) Station 2

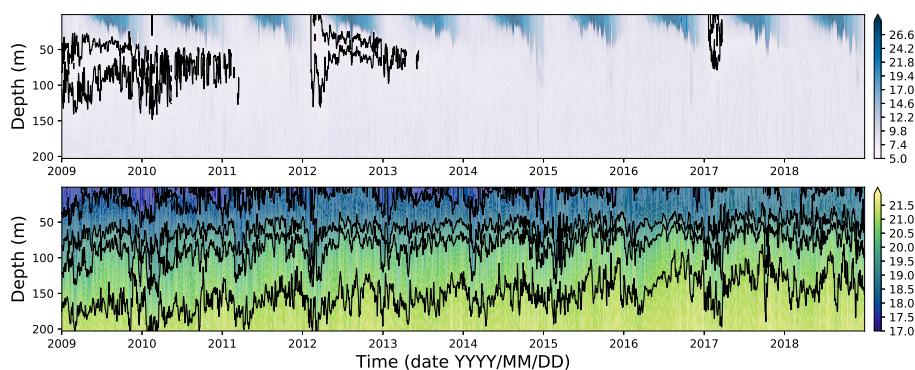


**Figure 14.** Time series of temperature and salinity versus depth at (a) station 1 and (b) station 2 of Figure 1.

the deeper central basin and near the coast stand as evidence that great changes are occurring in the Black Sea, much likely to be an amplified response to climate change in the isolated Black Sea basin severely limited in its communication with the Mediterranean Sea and eventually with the world ocean.

## 5 Conclusions

- 5 In this study, a high resolution Black Sea model was developed, with additional merits of coupling the basin hydrodynamics with exchange flows at Bosphorus Strait, with an artificial box on the Marmara side where the temperature and salinity is relaxed to climatology on a daily basis and open boundary conditions allowing a net flow in tune with the net flow across the Strait and allowing two-layer outflows and inflows of the Marmara Sea. While previous modelling studies mostly used climatological inflow/outflow water transport specified at the Strait entrance as a riverine like input over the limited number of grid points,
- 10 this study includes the high frequency variations in the exchange flow while still satisfying the net water balance of the Black Sea achieved by extending the model domain to include part of the Marmara Sea and the Bosphorus Strait. The model results



were rigorously evaluated by comparing them with the huge number of ARGO float profiles and available tide gauge station observations in the Black Sea.

The detailed analysis of the monthly mean circulation revealed complex and rapidly changing eddy activity in the Black Sea. Model temperature and salinity results are in good agreement with observations during the investigated period. Slight increases of salinity detected by observations in the upper water column are also evident in the model results. Ten years of simulation of temperature and salinity do not show any significant drift, which is an important feature that would allow the model to be used for long-term climate change simulations. The main feature of the Black Sea oceanography such as CIL water mass, rim current, upwelling along the southern coast are all well detected by the newly developed model. The model was also able to reproduce the SSH variability in comparison with the tide gauge observations.

Although high frequency sea level variations seem to be well reproduced by the model, there appears some mismatch between the model and observation in the SSH estimates at seasonal time scales, generally amplified in summer season. The differences in seasonal SSH pattern could be due to some deficits in water budget based on climatological river fluxes and steric effects often not considered in models.

In the future, the Marmara box domain should be extended to include the north Aegean Sea which will enable to specify the SSH and baroclinic velocities from CMEMS-Mediterranean model at the open boundaries. It is expected that this will improve performance of the model. The current model has used the linear free surface option. Since we have only defined temperature and salinity over limited part of the Marmara Sea, the non-linear free surface option was found to generate higher velocities and instabilities at Strait entrances, eventually causing the model to blow-up. Extending the model domain and with proper open boundary conditions, it is believed that the model could produce better results in non-linear free surface mode. The behaviour of the model should also be investigated by conducting long term model runs, starting with initial conditions from 1992 till present time to evaluate climate change aspects.

*Data availability.* The data can be made available by contacting the authors.

*Code and data availability.* BSEA is a regional configuration of NEMO (Nucleus for European Models of the Ocean) at version 4. stable (Madec, 2016). Model code is freely available from the NEMO website ([www.nemo-ocean.eu](http://www.nemo-ocean.eu)). After registration the Fortran code is readily available using the open-source subversion software (<http://subversion.apache.org>). There is only minor change over the original code. The friction was artificially increased over the Bosphorus Strait grid points.

*Author contributions.* MG, EO and RH set-up the NEMO model for the Black Sea. MG and EO performed the experiment. MG,EO and RH analyzed the model results. MG compare the model results with the observations. MG and EO wrote the paper with the inputs from all coauthors.



*Competing interests.* The authors declare that they have no conflict of interest.

*Acknowledgements.* Murat Gunduz was supported by the Scientific and Technological Research Council of Turkey (TUBITAK) (Project number: 114Y851). During the course this study we have obtained valuable help from various colleagues. An early version of the model configuration based on NEMO version 3.1 had been initially set up by Nathalie Toque; the objective analyses of whole-basin temperature and salinity data to set up Black Sea initial conditions was carried out with help from Mayotte Patron and Hazem Nagy; help in designing the model grid and smoothing the topography was kindly provided by Adil Sözer. We have made efficient use of computer facilities at our affiliated institutions for the computations and those at the ECMWF to obtain surface atmospheric data from MARS archives, in order to construct model forcing. Our special thanks are due to few functionaries of the establishment who unintentionally strengthened the collaboration that made this study possible despite several breaks.



## References

- Altıok, H. and Kayıçoğlu, M.: Seasonal and interannual variability of water exchange in the Strait of Istanbul, *Mediterranean Marine Science*, 16, 644–655, 2015.
- Arkipkin, V. S. and Bereznoi, V. Y.: Steric oscillations of the Black Sea level, *Oceanology*, 35, 735–741, 1995.
- 5 Aydoğdu, A., Hoar, T., Vukicevic, T., Anderson, J. L., Pinardi, N., Karspeck, A., Hendricks, J., Collins, N., Macchia, F., and Özsoy, E.: OSSE for a sustainable marine observing network in the Sea of Marmara, *Nonlinear Processes in Geophysics*, 2018a.
- Aydoğdu, A., Pinardi, N., Özsoy, E., Danabaşoğlu, G., Gürses, Ö., and Karspeck, A.: Circulation of the Turkish Straits System under interannual atmospheric forcing, *Ocean Science*, 2018b.
- Beşiktepe, Ş., Özsoy, E., and Ünlüata, Ü.: Filling of the Marmara Sea by the Dardanelles lower layer inflow, *Deep Sea Research Part I: Oceanographic Research Papers*, 40, 1815–1838, 1993.
- 10 Beşiktepe, Ş. T., Sur, H. İ., Özsoy, E., Latif, M. A., Oğuz, T., and Ünlüata, Ü.: The circulation and hydrography of the Marmara Sea, *Progress in Oceanography*, 34, 285–334, 1994.
- Blanke, B. and Delecluse, P.: Variability of the tropical Atlantic Ocean simulated by a general circulation model with two different mixed-layer physics, *Journal of Physical Oceanography*, 23, 1363–1388, 1993.
- 15 Bondar, C.: Considerations on water balance of the Black Sea. Report on the chemistry of seawater, in: *Proceedings of the XXXIII International Conference on Chemical and Physical Oceanography of the Black Sea*, pp. 2–4, 1986.
- Delfanti, R., Özsoy, E., Kaberi, H., Schirone, A., Salvi, S., Conte, F., Tsabaris, C., and Papucci, C.: Evolution and fluxes of  $^{137}\text{Cs}$  in the black sea/turkish straits system/north aegean sea, *Journal of Marine Systems*, 135, 117–123, 2014.
- Dorrell, R. M., Peakall, J., Sumner, E., Parsons, D., Darby, S., Wynn, R., Özsoy, E., and Tezcan, D.: Flow dynamics and mixing processes in hydraulic jump arrays: Implications for channel-lobe transition zones, *Marine Geology*, 381, 181–193, 2016.
- 20 Dorrell, R. M., Peakall, J., Darby, S. E., Parsons, D. R., Johnson, J., Sumner, E. J., Wynn, R. B., Özsoy, E., and Tezcan, D.: Self-sharpening induces jet-like structure in seafloor gravity currents, *Nature communications*, 10, 1381, 2019.
- Falina, A., Sarafanov, A., Özsoy, E., and Turunçoğlu, U. U.: Observed basin-wide propagation of Mediterranean water in the Black Sea, *Journal of Geophysical Research: Oceans*, 122, 3141–3151, 2017.
- 25 Farmer, D. M. and Armi, L.: Maximal two-layer exchange over a sill and through the combination of a sill and contraction with barotropic flow, *Journal of Fluid Mechanics*, 164, 53–76, 1986.
- Farmer, D. M. and Armi, L.: The flow of Atlantic water through the Strait of Gibraltar, *Progress in Oceanography*, 21, 1–103, 1988.
- Gregg, M. C. and Özsoy, E.: Flow, water mass changes, and hydraulics in the Bosphorus, *Journal of Geophysical Research: Oceans*, 107, 2002.
- 30 Gregg, M. C., Özsoy, E., and Latif, M. A.: Quasi-steady exchange flow in the Bosphorus, *Geophysical Research Letters*, 26, 83–86, 1999.
- Grinevetsky, S. R., Zonn, I. S., Zhiltsov, S. S., Kosarev, A. N., and Kostianoy, A. G.: *The Black Sea Encyclopedia*, "Springer Berlin Heidelberg", 2002.
- Ilicak, M., Özgökmen, T. M., Özsoy, E., and Fischer, P. F.: Non-hydrostatic modeling of exchange flows across complex geometries, *Ocean Modelling*, 29, 159–175, 2009.
- 35 Jarosz, E., Teague, W. J., Book, J. W., and Beşiktepe, Ş.: On flow variability in the Bosphorus Strait, *Journal of Geophysical Research: Oceans*, 116, 2011a.



- Jarosz, E., Teague, W. J., Book, J. W., and Beşiktepe, Ş.: Observed volume fluxes in the Bosphorus Strait, *Geophysical Research Letters*, 38, 2011b.
- Kelley, D. E., Fernando, H. J. S., Gargett, A. E., Tanny, J., and Özsoy, E.: The diffusive regime of double-diffusive convection, *Progress in Oceanography*, 56, 461–481, 2003.
- 5 Kosarev, A. N.: *The Black Sea Environment*, vol. 5, Springer, 2007.
- Latif, M. A., Özsoy, E., Oğuz, T., and Ünlüata, Ü.: Observations of the Mediterranean inflow into the Black Sea, *Deep Sea Research Part A. Oceanographic Research Papers*, 38, S711–S723, 1991.
- Madec, G.: NEMO ocean engine, Note du Pole de modélisation, Institut Pierre-Simon Laplace (IPSL), France, No 27, Tech. rep., ISSN-1288-1619, 2008.
- 10 Murray, J. W., Top, Z., and Özsoy, E.: Hydrographic properties and ventilation of the Black Sea, *Deep Sea Research Part A. Oceanographic Research Papers*, 38, S663–S689, 1991.
- Oddo, P. and Pinardi, N.: Lateral open boundary conditions for nested limited area models: a scale selective approach, *Ocean Modelling*, 20, 134–156, 2008.
- Oğuz, T. and Malanotte-Rizzoli, P.: Seasonal variability of wind and thermohaline-driven circulation in the Black Sea: Modeling studies, *Journal of Geophysical Research: Oceans*, 101, 16 551–16 569, 1996.
- 15 Oğuz, T., Latun, V. S., Latif, M. A., Vladimirov, V. V., Sur, H. İ., Markov, A. A., Özsoy, E., Kotovshchikov, B. B., Ereemeev, V. V., and Ünlüata, Ü.: Circulation in the surface and intermediate layers of the Black Sea, *Deep Sea Research Part I: Oceanographic Research Papers*, 40, 1597–1612, 1993.
- Oğuz, T., Tuğrul, S., Kıdeys, A. E., Ediger, V., and Kubilay, N.: Physical and biogeochemical characteristics of the Black Sea, *The Sea*, 14, 20 1331–1369, 2005.
- Özsoy, E. and Altıok, H.: A review of hydrography of the Turkish Straits System, *The Sea of*, p. 13, 2016a.
- Özsoy, E. and Altıok, H.: A review of water fluxes across the Turkish Straits System, *The Sea of*, p. 42, 2016b.
- Özsoy, E. and Beşiktepe, Ş.: Sources of double diffusive convection and impacts on mixing in the Black Sea, *Washington DC American Geophysical Union Geophysical Monograph Series*, 94, 261–274, 1995.
- 25 Özsoy, E. and Ünlüata, Ü.: Oceanography of the Black Sea: a review of some recent results, *Earth-Science Reviews*, 42, 231–272, 1997.
- Özsoy, E. and Ünlüata, Ü.: The Black Sea, *The Sea*, 11, 889–914, 1998.
- Özsoy, E., Top, Z., White, G., and Murray, J. W.: Double diffusive intrusions, mixing and deep sea convection processes in the Black Sea, in: *Black Sea Oceanography*, pp. 17–42, Springer, 1991.
- Özsoy, E., Ünlüata, Ü., and Top, Z.: The Mediterranean water evolution, material transport by double diffusive intrusions, and interior mixing 30 in the Black Sea, *Progress in Oceanography*, 31, 275–320, 1993.
- Özsoy, E., Latif, M. A., Tuğrul, S., and Ünlüata, Ü.: Exchanges with the Mediterranean, fluxes and boundary mixing processes in the Black Sea, *Bulletin del Institut Océanographique. Mediterranean Tributary Seas*, Monaco, pp. 1–25, 1995.
- Özsoy, E., Latif, M. A., Sur, H. İ., and Goryachkin, Y.: A review of the exchange flow regime and mixing in the Bosphorus Strait, *Bulletin-Institut Oceanographique Monaco-Numero Special*, pp. 187–204, 1996.
- 35 Özsoy, E., Di Iorio, D., Gregg, M. C., and Backhaus, J. O.: Mixing in the Bosphorus Strait and the Black Sea continental shelf: observations and a model of the dense water outflow, *Journal of Marine Systems*, 31, 99–135, 2001.
- Özsoy, E., Rank, D., and Salihoglu, İ.: Pycnocline and deep mixing in the Black Sea: stable isotope and transient tracer measurements, *Estuarine, Coastal and Shelf Science*, 54, 621–629, 2002.



- Özsoy, E., Çagatay, M., Balkis, N., Balkis, N., and Öztürk, B.: The Sea of Marmara; Marine Biodiversity, Fisheries, Conservation and Governance, Turkish Marine Research Foundation (TUDAV), Publication, 2016.
- Rank, D., Özsoy, E., and Salihoğlu, İ.: Oxygen-18, deuterium and tritium in the Black Sea and the Sea of Marmara, *Journal of Environmental Radioactivity*, 43, 231–245, 1999.
- 5 Sannino, G., Sözer, A., and Özsoy, E.: Recent advancements on modelling the exchange flow dynamics through the Turkish Straits System, *Black Sea/Mediterranean Environment*, p. 110, 2014.
- Sannino, G., Sözer, A., and Özsoy, E.: A high-resolution modelling study of the Turkish Straits System, *Ocean Dynamics*, 67, 397–432, 2017.
- Sarkisyan, A. S. and Sündermann, J. E.: *Modelling Climate Variability of Selected Shelf Seas*, Springer, 2009.
- 10 Simonov, A. and Altman, E.: Hydrometeorology and hydrochemistry of seas of USSR. IV, Black Sea, pt. 1, Hydrometeorological conditions, 1991.
- Song, Y. and Haidvogel, D.: A semi-implicit ocean circulation model using a generalized topography-following coordinate system, *Journal of Computational Physics*, 115, 228–244, 1994.
- Sorokin, I.: *The Black Sea: Ecology and Oceanography, Biology of inland waters*, Backhuys Pub., 2002.
- 15 Sözer, A. and Özsoy, E.: Modeling of the Bosphorus exchange flow dynamics, *Ocean dynamics*, 67, 321–343, 2017a.
- Sözer, A. and Özsoy, E.: Water Exchange through Canal İstanbul and Bosphorus Strait, *Mediterranean Marine Science*, 18, 77–86, 2017b.
- Stanev, E., Grashorn, S., and Zhang, Y.: Cascading ocean basins: numerical simulations of the circulation and interbasin exchange in the Azov-Black-Marmara-Mediterranean Seas system., *Ocean Dynamics*, 67, 2017.
- Stanev, E. V.: On the mechanisms of the Black Sea circulation, *Earth-Science Reviews*, 28, 285–319, 1990.
- 20 Sur, H. İ., Özsoy, E., and Ünlüata, Ü.: Boundary current instabilities, upwelling, shelf mixing and eutrophication processes in the Black Sea, *Progress in Oceanography*, 33, 249–302, 1994.
- Sur, H. İ., Özsoy, E., Ilyin, Y. P., and Ünlüata, Ü.: Coastal/deep ocean interactions in the Black Sea and their ecological/environmental impacts, *Journal of Marine Systems*, 2, 293–320, 1996.
- Tsimplis, M., Josey, S., Rixen, M., and Stanev, E.: On the forcing of sea level in the Black Sea, *Journal of Geophysical Research: Oceans*, 25 109, 2004.
- Ünlüata, Ü., Oğuz, T., Latif, M. A., and Özsoy, E.: On the physical oceanography of the Turkish Straits, in: *The physical oceanography of sea straits*, pp. 25–60, Springer, 1990.
- Vespremeanu, E. and Golumbeanu, M.: *The Black Sea: Physical, Environmental and Historical Perspectives*, Springer, 2017.